Journal of Solid State Chemistry **164,** 163–168 (2002)
doi:10.1006/jssc.2001.9467, available online at http://www.idealibrary.com on IDEAL®

Magnetic and Calorimetric Studies on One-Dimensional Ln_3RuO_7 (Ln = Pr, Gd)

Daijitsu Harada and Yukio Hinatsu

Division of Chemistry, Graduate School of Science, Hokkaido University, Sapporo 060-0810, Japan

Received May 15, 2001; in revised form November 2, 2001; accepted November 30, 2001

Magnetic and calorimetric properties of Ln_3RuO_7 (Ln = Pr, Gd) have been investigated. Magnetic susceptibility and specific heat measurements indicate that both Pr_3RuO_7 and Gd_3RuO_7 compounds show magnetic transitions at 55 K and 15 K, respectively. In addition, a clear structural phase transition has been found at 382 K for Gd_3RuO_7 from the specific heat measurements. From the temperature dependence of the magnetic specific heat, the magnetic entropy change is estimated and the magnetic ground states of each ion are determined. © 2002 Elsevier Science (USA)

1. INTRODUCTION

Ruthenium-based oxides have recently been of interest because of their unusual electronic and magnetic properties. Among them, we have focused our attention on a series of ruthenates Ln_3RuO_7 (Ln = lanthanides) (1, 2). They are part of a large family of chain compounds with the formula Ln_3MO_7 (M = pentavalent 4*d*, 5*d* transition metal cations). In this case, the cations, which are of significantly different radii, order in a 2_{Ln}:1_{Ln}:1_M pattern over the f.c.c. fluorite cation sites. The existence of the Ln_3MO_7-type compounds was first reported by Allpress and Rossell (3). Rossell determined the precise crystal structure of La_3NbO_7 in 1979 (4). For large Ln cations, an orthorhombic fluorite-related superstructure is found, while for the smaller Ln cations, the structure is a defect fluorite type. In the superstructure, the M^{5+} cation is octahedrally coordinated by six oxygen ions and the MO_6 octahedra share corners, forming a zig-zag one-dimensional chain. The interchain M–M distance is about 6.6 Å compared with the corresponding intrachain distance of 3.7 Å, which suggests that these compounds may exhibit one-dimensional electronic behavior.

Van Berkel and IJdo first described lanthanide ruthenates Ln_3RuO_7 (5) and Groen *et al.* determined the precise structure of Nd_3RuO_7 (6). All the Ln_3RuO_7-type compounds reported until now (Ln = La, Pr, Nd, Sm, Eu, Gd) are orthorhombic with space group *Cmcm*.

Recently, measurements of the physical properties of Ln_3RuO_7 have been carried out. Khalifah *et al.* investigated electronic and magnetic properties of La_3RuO_7 through its neutron diffraction, electrical resistivity, and magnetic susceptibility measurements, and the band structure calculations (7, 8). La_3RuO_7 is a semiconductor and it transforms to an antiferromagnetic state at $T_N = 17$ K. Wiss *et al.* investigated the magnetic properties of Pr_3RuO_7 (9) and found that Pr_3RuO_7 is also antiferromagnetic below $T_N = 50$ K. Bontchev *et al.* successfully prepared for the first time Gd_3RuO_7 and determined the crystal structure at room temperature from single crystals (10). They observed two antiferromagnetic transitions at 8.0 and 14.5 K for Gd_3RuO_7.

Previously, we studied crystal structures and magnetic and calorimetric properties for Ln_3RuO_7 (Ln = Nd, Sm, Eu) (1, 2). Antiferromagnetic transitions with weak ferromagnetic components have been observed at 19.0, 22.5, and 22.5 K for Ln_3RuO_7 (Ln = Nd, Sm, and Eu, respectively). We have also found structural phase transitions for Ln_3RuO_7 (Ln = Nd, Sm, and Eu) at 130, 190, and 280 K, respectively. Neutron diffraction measurements on Nd_3RuO_7 indicate that its orthorhombic crystal structure (space group *Cmcm*) transform to the monoclinic structure with space group $P2_1/m$ below the transition temperature (2).

In this study, we have extended our studies on the magnetic and calorimetric properties of Ln_3RuO_7 to Pr_3RuO_7 and Gd_3RuO_7. Two compounds, Pr_3RuO_7 and Gd_3RuO_7, were prepared, and their susceptibility and specific heat were measured. Including previous results on Ln_3RuO_7, we attempt to characterize the physical properties of Ln_3RuO_7 compounds and comment on their crystal structures.

2. EXPERIMENTAL

As starting materials, Pr_6O_{11} (99.9%), Gd_2O_3 (99.9%), and RuO_2 (99.9%) were used. These reagents were obtained

0022-4596/02 $35.00

from Nihon Yttrium Co. Ltd. (for Pr_6O_{11} and Gd_2O_3) and Soekawa Chemical Co. Ltd. (for RuO_2). They were weighed in appropriate metal ratios and the mixtures were ground in an agate mortar, pressed into pellets, and reacted in air at 1200°C for 12–48 h with several interval grindings.

Powder X-ray diffractometry was carried out for Pr_3RuO_7 and Gd_3RuO_7 in the region of $10^\circ \leq 2\theta \leq 120^\circ$ in increments of 0.02° (2θ) at the scanning speed of 250 sec/° at room temperature with a Rigaku MultiFlex using Cu$K\alpha$ radiation. Their crystal structures were refined with the Rietveld method, using the Rietan-2000 program (11).

Magnetic susceptibilities were measured using SQUID magnetometer (Quantum Design, Model MPMS-5S) from 2.0 to 350 K (from 1.8 to 400 K for Gd_3RuO_7). The magnetic susceptibility was measured under both zero-field-cooled conditions (ZFC) and field-cooled conditions (FC). The former was measured upon heating the sample to 350 K under the applied magnetic field of 0.1 T after zero-field cooling to 2.0 K. The latter was measured upon cooling the sample from 350 to 2.0 K at 0.1 T.

The specific heat measurements were performed using a relaxation technique supplied by the commercial specific heat measurement system (Quantum Design, PPMS) in the temperature range $2.0\ \text{K} \leq T \leq 300\ \text{K}$ for Pr_3RuO_7 and in the temperature range $1.8\ \text{K} \leq T \leq 400\ \text{K}$ for Gd_3RuO_7. The sample in the form of a pellet was mounted on an aluminum plate with apiezon for better thermal contact.

3. RESULTS AND DISCUSSION

3.1. Crystal Structures for Ln_3RuO_7 at Room Temperature

Figure 1 shows the powder X-ray diffraction profiles for Ln_3RuO_7 (Ln = Pr, Nd, Sm, Eu, Gd) in the angle range $10^\circ \leq 2\theta \leq 120^\circ$. No reflection forbidden for a C lattice is observed. Table 1 lists the lattice parameters and atomic positions for Pr_3RuO_7 which were refined in the space group $Cmcm$. These values are in good agreements with those reported by Wiss *et al.* (9). Figure 2 illustrates the crystal structure of Pr_3RuO_7. The characteristic feature of this structure is that slabs are formed in the bc-plane, in which a one-dimensional RuO_6 chain runs parallel to the c-axis alternately with rows of edge-shared LnO_8 pseudocubes composed of one-third of the Ln ions. These slabs are separated by the remaining two-thirds of the Ln ions which are seven-coordinated by oxygen ions. Therefore, we can expect to find the magnetic interactions between Ru^{5+} ions in a chain and further the interactions between Ru^{5+} and Ln^{3+} ions. The structure of Gd_3RuO_7 is basically the same as that of Pr_3RuO_7.

TABLE 1
Crystal Structure Data for Pr_3RuO_7 at Room Temperature from Powder X-Ray Diffraction

Atom	Position	x	y	z	B (Å^2)
Space group $Cmcm$ (No. 63)					
$Z = 4$; $a = 10.9806(2)$ Å, $b = 7.3841(1)$ Å, $c = 7.5311(1)$ Å; $V = 610.63(2)$ Å^3					
$R_{wp} = 14.35\%$; $R_e = 8.69\%$; $R_I = 2.11\%$					
Pr1	4a	0.0	0.0	0.0	0.59(5)
Pr2	8g	0.2221(2)	0.3124(1)	0.25	0.25(3)
Ru	4b	0.0	0.5	0.0	0.17(5)
O1	16h	0.126(1)	0.319(2)	− 0.042(2)	0.14(9)
O2	8g	0.130(2)	0.030(3)	0.25	0.14(9)
O3	4c	0.0	0.424(4)	0.25	0.14(9)

Note. Definitions of reliability factors R_{wp}, R_e, and R_I are given as follows: $R_{\text{wp}} = [\sum_i w_i(y_i - f_i(x))^2 / \sum_i w_i y_i^2]^{1/2}$, $R_{\text{e}} = [N_{\text{o}} - N_{\text{r}} - N_{\text{c}} / \sum_i w_i y_i^2]^{1/2}$, and $R_1 = [\sum_k [I_k(\text{obs}) - I_k(\text{calc})| / \sum_k \text{I}_k(\text{obs})]$.

3.2. Magnetic and Calorimetric Properties for Gd_3RuO_7

Figure 3 shows the temperature dependence of the magnetic susceptibility for Gd_3RuO_7. An antiferromagnetic

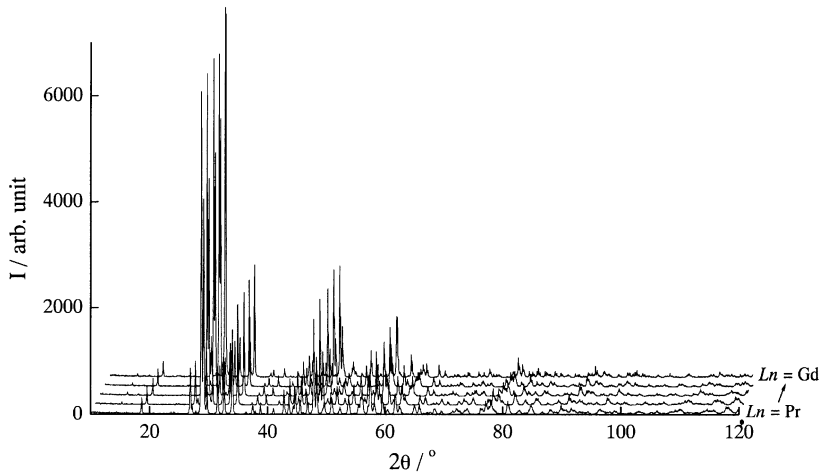

FIG. 1. Powder X-ray diffraction profiles for Ln_3RuO_7 (Ln = Pr, Nd, Sm, Eu, Gd).

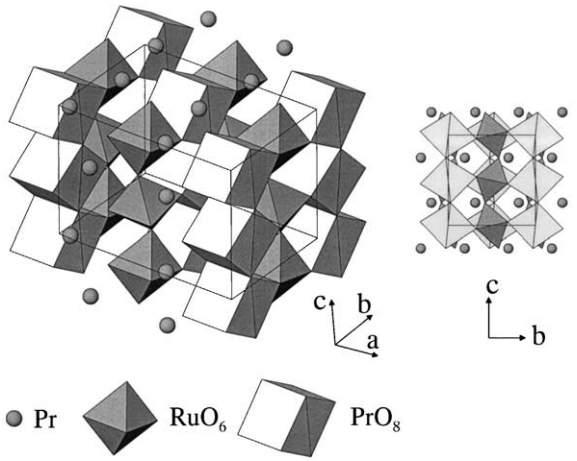

FIG. 2. Crystal structure of Pr_3RuO_7.

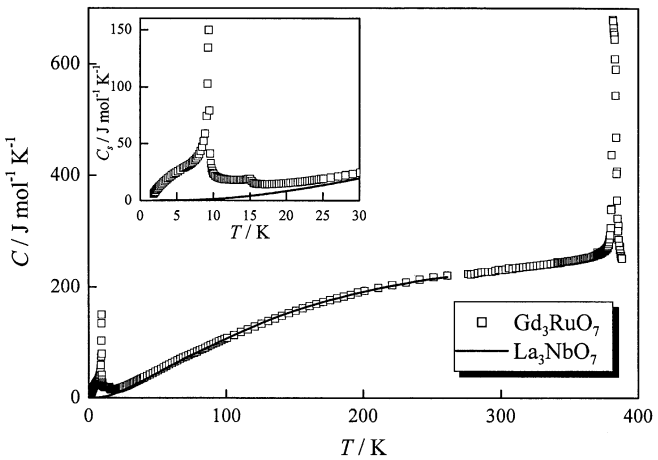

FIG. 4. Temperature dependence of specific heat for Gd_3RuO_7 in the range 1.8 K $\leq T \leq$ 400 K. The inset shows the detailed temperature dependence in the range 1.8 K $\leq T \leq$ 30 K. The specific heat of La_3NbO_7 is shown with a solid line (see text).

transition occurs at 15 K and the divergence between the ZFC and FC susceptibilities is observed below 9.5 K, which is in agreement with the previous result reported by Bontchev *et al.* (10). In the temperature range above 200 K, the Curie–Weiss law holds. The Curie constant and Weiss constant are determined to be $C_{Gd_3RuO_7} = 23.63$ emu K mol^{-1} and $\theta = -26$ K, respectively. The Curie constant expected for Gd_3RuO_7 is calculated to be $C_{Gd_3RuO_7} =$ 23.53 emu K mol^{-1} by substituting the theoretical magnetic moments of the free ions, $\mu_{Gd^{3+}} = 7.94\,\mu_B$ and $\mu_{Ru^{5+}} =$ 3.87 μ_B, into the equation, $C_{Gd_3RuO_7} = 3C_{Gd^{3+}} + C_{Ru^{5+}}$. The observed Curie constant is close to the calculated one. This result indicates that there are no magnetic interactions between moments of Ru^{5+} and Gd^{3+} ions in the paramagnetic temperature region.

Figure 4 shows the temperature dependence of the specific heat for Gd_3RuO_7. Two distinct specific heat anomalies

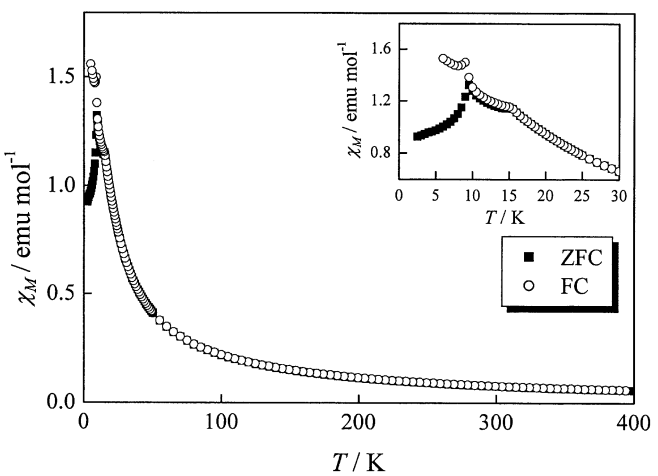

FIG. 3. Temperature dependence of magnetic susceptibility for Gd_3RuO_7 in the range 2 K $\leq T \leq$ 400 K. The inset shows the detailed temperature dependence in the range 2 K $\leq T \leq$ 30 K.

are found at 9.5 K and 382 K. The λ-type anomaly at lower temperature, 9.5 K, corresponding to the second-order transition, indicates the occurrence of the magnetic transition at this temperature. This is consistent with the results obtained by the magnetic suscceptibility measurements (see Fig. 3). In addition, a small specific heat anomaly is also observed at 15 K (see the inset of Fig. 4), which is also in accordance with the anomaly found in the susceptibility vs temperature curve (see Fig. 3). On the other hand, the shape of the anomaly at higher temperature, 382 K, is characteristic of the first-order transition.

Previously, we reported the first-order transitions for Ln_3RuO_7 (Ln = Nd, Sm, and Eu) at 130 K, 190 K, and 280 K, respectively (1, 2). Neutron diffraction measurements for Nd_3RuO_7 at lower temperatures indicated that this transition is a monoclinic (space group $P2_1/m$)–orthorhombic (space group $Cmcm$) structural phase transition (2). The phase transition temperature increases with decreasing ionic radius of Ln^{3+}, and the transition temperature for Gd_3RuO_7, 382 K, follows this trend. It is the highest among Ln_3RuO_7. Therefore, the phase of Gd_3RuO_7 at room temperature should be a low-temperature monoclinic phase, which is inconsistent with the results reported by Bontchev *et al.* (10). The nature of the phase transition at 382 K needs further research.

Next, we will estimate the magnetic entropy change associated with the antiferromagnetic interactions from the specific heat data. To calculate the magnetic contribution to the specific heat, we have to subtract the electronic and lattice contributions from the total specific heat. To estimate them, we prepared a diamagnetic compound, La_3NbO_7, which is isomorphous with Gd_3RuO_7 and measured its specific heat. In Fig. 4, the specific heat data of La_3NbO_7 are also shown.

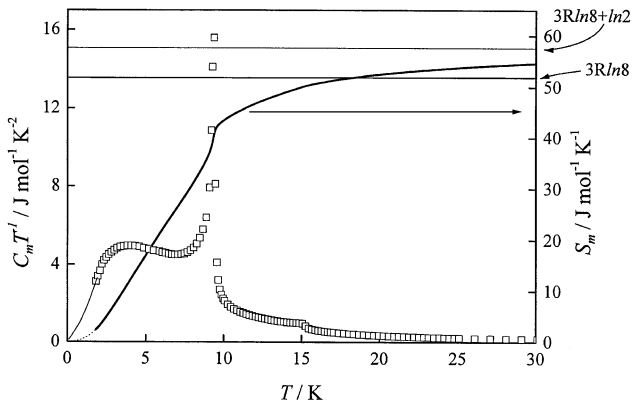

FIG. 5. The C_m/T (left ordinate) and the magnetic entropy change (right ordinate) versus temperature for Gd_3RuO_7.

If we assume that the electronic and lattice contributions to the specific heat are equal between Gd_3RuO_7 and La_3NbO_7, the magnetic specific heat (C_m) for Gd_3RuO_7 is obtained by subtracting the specific heat of La_3NbO_7. Figure 5 shows the magnetic specific heat of Gd_3RuO_7 divided by temperature (C_m/T) and the magnetic entropy change (S_m) as a function of temperature. A dashed line represents the extrapolated magnetic specific heat below 1.8 K. This is calculated by fitting the magnetic specific heat to the function $f(T) = aT^3$ in the temperature range $1.8\ \mathrm{K} \leq T \leq 3.0\ \mathrm{K}$, which is based on the antiferromagnetic spin-wave model (12). The magnetic entropy change associated with the antiferromagnetic transition is calculated by integrating $S_m(T) = \int (C_m/T)\,dT$, and it is close to about $56\ \mathrm{J\,mol^{-1}\,K^{-1}}$, although a slight increase is observed with increasing temperature. The octet-degenerate $^8S_{7/2}$ for the ground state of Gd^{3+} ion is not split even by the low-symmetric crystal field. Therefore, the following magnetic entropy is attained in principle just above the ordering temperature,

$$R\ln(2S+1) = R\ln(2\cdot 7/2+1) = R\ln 8,$$

where R is a molar gas constant. On the other hand, the magnetic entropy change with the ordering of Ru^{5+} ions in these Ln_3RuO_7 compounds is estimated to be $R\ln 2$ (1, 2). In the case that all the magnetic ions in the Gd_3RuO_7 are ordered, the expected magnetic entropy change is calculated to be

$$3\ R\ln 8 + R\ln 2 = 57.2\ \mathrm{J\,mol^{-1}\,K^{-1}},$$

which is in good accordance with the observed one. Most of the magnetic entropy change occurs below 9.5 K (see Fig. 5), which indicates that the magnetic ordering of the Gd^{3+} ions occurs below this temperature. Therefore, we consider that when the temperature is decreased to 15 K, the magnetic moments of Ru^{5+} ions begin to order and below 9.5 K, the ordering of the magnetic moments of Gd^{3+} ions proceeds rapidly. In the case that Gd^{3+} ions are ordered, the internal magnetic field leads to the Zeeman splitting, which causes the Schottky-type specific heat anomaly for compounds including Gd^{3+} ions. And it is often reported that a lower-temperature broad shoulder appears below the transition temperature in the specific heat vs temperature curve (13, 14). In the present study, the shoulder appears around 4 K in the specific heat vs temperature curve. This fact also supports that Gd^{3+} ions are ordered below 9.5 K.

3.3. *Magnetic and Calorimetric Properties for Pr_3RuO_7*

Figure 6 shows the temperature dependence of the magnetic susceptibility for Pr_3RuO_7, indicating that an antiferromagnetic transition occurs at 55 K. This transition temperature agrees with the report by Wiss *et al.* (9). There is no divergence between the ZFC and FC susceptibilities. A small magnetic anomaly is observed around 35 K. We estimated a Curie constant (C) and a Weiss constant (θ) in the temperature range above 200 K in which the Curie–Weiss law holds. They are determined to be $C_{Pr_3RuO_7} = 5.90\ \mathrm{emu\ K\ mol^{-1}}$ and $\theta = 2.2$ K. These values are close to those reported previously (9), $C_{Pr_3RuO_7} = 5.96\ \mathrm{emu\ K\ mol^{-1}}$ and $\theta = 11$ K. The Curie constant expected for Pr_3RuO_7 is calculated to be $C_{Pr_3RuO_7} = 6.69\ \mathrm{emu\ K\ mol^{-1}}$ by substituting the theoretical magnetic moments of the free ions, $\mu_{Pr^{3+}} = 3.58\ \mu_B$ and $\mu_{Ru^{5+}} = 3.87\ \mu_B$ into the equation, $C_{Pr_3RuO_7} = 3C_{Pr^{3+}} + C_{Ru^{5+}}$. The observed Curie constant is smaller than the calculated one, which suggests that the magnetic ions in this compound may be affected by the crystal field to some extent.

The temperature dependence of specific heat for Pr_3RuO_7 is shown in Fig. 7. A λ-type anomaly is observed at 55 K and

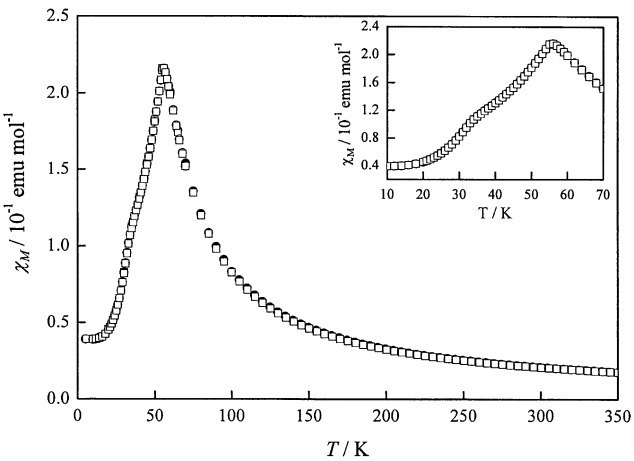

FIG. 6. Temperature dependence of magnetic susceptibility for Pr_3RuO_7 in the range $2\ \mathrm{K} \leq T \leq 350\ \mathrm{K}$. The inset shows the detailed temperature dependence in the range $10\ \mathrm{K} \leq T \leq 70\ \mathrm{K}$.

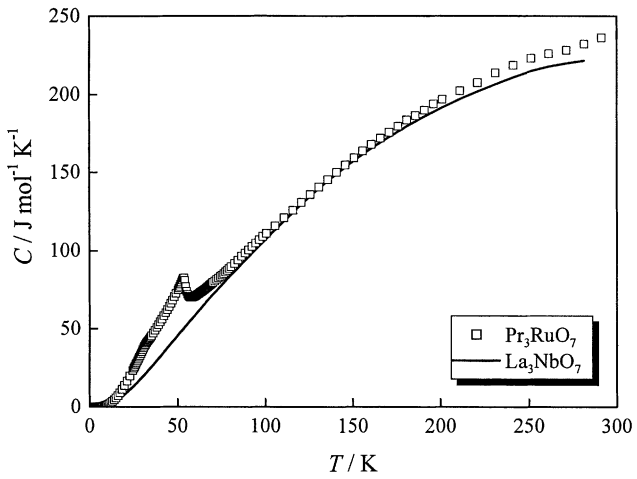

FIG. 7. Temperature dependence of specific heat for Pr_3RuO_7 in the range 1.8 K $\leq T \leq$ 300 K. The specific heat of La_3NbO_7 is shown with a solid line.

another small anomaly is found around 35 K. These anomalies are in accordance with the results by the magnetic susceptibility measurements. To calculate the magnetic contribution to the specific heat, we used the specific heat data for La_3NbO_7, and have assumed that the electronic and lattice contributions to the total specific heat are equal between Pr_3RuO_7 and La_3NbO_7. Figure 8 shows the magnetic specific heat of Pr_3RuO_7 divided by temperature (C_m/T) and the magnetic entropy change (S_m) as a function of temperature. This figure indicates that the magnetic entropy change for the antiferromagnetic transition of Pr_3RuO_7 at 55 K is ca. 25 J mol^{-1} K^{-1}. Since the precise estimation of the lattice specific heat contribution to the total specific heat is difficult because of its high transition temperature, this value may involve some uncertainty. Indeed, the specific heat for La_3NbO_7 is considered to be

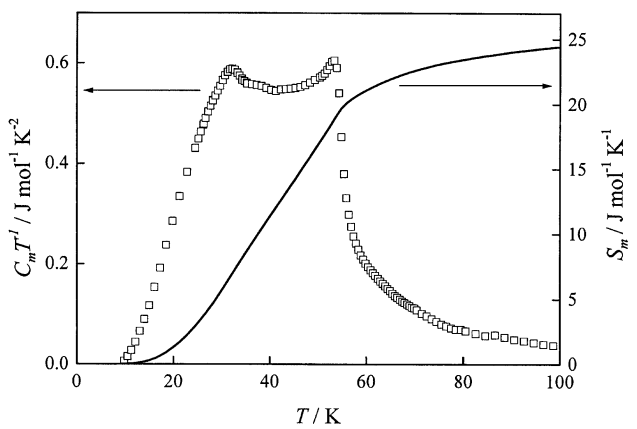

FIG. 8. The C_m/T (left ordinate) and the magnetic entropy change (right ordinate) versus temperature for Pr_3RuO_7.

lower than the total of the lattice and electronic specific heats (see Fig. 7). The maximum magnetic entropy change for the ordering of magnetic moments of Ru^{5+} ions (with a total spin quantum number $S = 3/2$) is estimated to be

$$R \ln (2S + 1) = R \ln(2 \cdot 3/2 + 1) = R \ln 4$$
$$(= 11.52 \text{ J mol}^{-1} \text{K}^{-1}).$$

The magnetic entropy change observed is much larger than this value, indicating that the magnetic moments of Pr^{3+} ions as well as those of Ru^{5+} ions should have ordered.

Although most of the Ln_3RuO_7 compounds show magnetic transitions at 15–22.5 K, the transition temperature for Pr_3RuO_7 is relatively high, 55 K. In addition, the magnetic behavior below the magnetic transition temperature for Pr_3RuO_7 is quite different from that for the other Ln_3RuO_7 compounds; i.e., there is no divergence between the ZFC and FC magnetic susceptibilities for Pr_3RuO_7, while the other Ln_3RuO_7 compounds show great divergence between the ZFC and FC susceptibilities. These differences in the magnetic behavior between Pr_3RuO_7 and the other Ln_3RuO_7 compounds suggest that the mechanism of the magnetic exchange interactions is different between them. We believe that the magnetic interactions between two Ru^{5+} ions are dominant for any Ln_3RuO_7 compound, and that the interactions between the Pr^{3+} and Ru^{5+} ions are also important in the Pr_3RuO_7. Wiss *et al.* also discussed the magnetic interactions of Ln_3RuO_7 compounds, using the Weiss constant (9), and they led to the same result as ours.

4. SUMMARY

In this study, magnetic and calorimetric properties of Pr_3RuO_7 and Gd_3RuO_7 have been investigated. Specific heat measurements for Gd_3RuO_7 show a structural phase transition at 382 K. Such a phase transition has been observed for Ln_3RuO_7 (Ln = Nd, Sm, Eu, and Gd) and their phase transition temperatures increase with decreasing ionic radius of Ln^{3+}.

Magnetic transitions have been observed for any Ln_3RuO_7 (Ln = Pr, Nd, Sm, Eu, Gd) compound. For Ln_3RuO_7 (Ln = Nd, Sm, Eu, Gd), the magnetic transitions occur at 15–22.5 K, while the magnetic transition temperature for Pr_3RuO_7 is much higher, 55 K. We consider that in addition to the magnetic interactions between Ru^{5+} ions, those between Ru^{5+} and Pr^{3+} ions are also important in the magnetic exchange mechanism of Pr_3RuO_7.

ACKNOWLEDGMENTS

This work was supported by the Suhara Memorial Foundation.

REFERENCES

1. D. Harada and Y. Hinatsu, *J. Solid State Chem.* **158,** 245 (2001).
2. D. Harada and Y. Hinatsu, *J. Phys.: Condens. Matter* **13,** 10825 (2001).
3. J. G. Allpress and H. J. Rossell, *J. Solid State Chem.* **27,** 105 (1979).
4. H. J. Rossell, *J. Solid State Chem.* **27,** 115 (1979).
5. F. P. F. van Berkel and D. J. W. IJdo, *Mater. Res. Bull.* **21,** 1103 (1986).
6. W. A. Groen, F. P. F. van Berkel, and D. J. W. IJdo, *Acta Crystallogr. C* **43,** 2262 (1986).
7. P. Khalifah, Q. Huang, J. W. Lynn, R. W. Erwin, and R. J. Cava, *Mater. Res. Bull.* **35,** 1 (2000).
8. P. Khalifah, R. W. Erwin, J. W. Lynn, Q. Huang, B. Batlogg, and R. J. Cava, *Phys. Rev. B* **60,** 9573 (1999).
9. F. Wiss, N. P. Raju, A. S. Wills, and J. E. Greedan, Inter. *J. Inorg. Mater.* **2,** 53 (2000).
10. B. P. Bontchev, A. J. Jacobson, M. M. Gospodinov, V. Skumryev, V. N. Popov, B. Lorenz, R. L. Meng, A. P. Litvinchuk, and M. N. Iliev, *Phys. Rev. B* **62,** 12235 (2000).
11. F. Izumi and T. Ikeda, *Mater. Sci. Forum* **198,** 321 (2000).
12. Y. J. Tang, X. W. Cao, J. C. Ho, and H. C. Ku, *Phys. Rev. B* **46,** 1213 (1991).
13. M. Bouvier, P. Lethullier, and D. Schmitt, *Phys. Rev. B* **43,** 13137 (1991).
14. Y. Y. Chen, C. C. Lai, B. S. Chiou, J. C. Ho, and H. C. Ku, *Phys. Rev. B* **47,** 12178 (1993).